(**H** parallel to the c axis) appears more strongly temperature-dependent than the mass of the lens orbit over the poles (**H** perpendicular to the c axis). A possible explanation for this is that the bare band masses for these orbits should be chosen somewhat differently. For example, if the estimated band mass of the orbit with **H** perpendicular to c were increased slightly, this would readjust the points in Fig. 4 upward, and could actually change the ordering of the two lens orbits. To resolve this question, we need either a band-structure mass calculation or a calculation of the enhancement $\lambda(O_k)$ for these orbits. It would be an interesting test of the pseudopotential model of electron-phonon coupling to attempt the detailed calculation of the mass enhancement for different orbits. Once the zero-temperature mass is calculated, there is no added difficulty in calculating the temperature dependence. The experimental knowledge of the low-temperature increase in $\lambda(T)$ then provides a useful extra check on the theory of the mass enhancement.

The experimental observation of the maximum in the mass enhancement as a function of temperature would be an interesting verification of the theory. Unfortunately, this is a difficult experiment at the present time, at least by the cyclotron-resonance method, because of temperature-dependent lifetime effects which prevent the observation of resonance at temperatures closer to the Debye temperature.

Note added in proof. Since submitting this paper, we have learned of several studies of the temperature dependence of the mass renormalization. Apparently the first was by Eliashberg[21] who pointed out the existence of a $T^2 \log T$ term in the electronic specific heat. Grimvall[22] has presented calculations similar to ours for $\lambda(T)$ in lead and mercury using experimental values of $\alpha^2(\omega)F(\omega)$. Appel[23] has studied the influence of this effect on the superconducting transition temperature.

ACKNOWLEDGMENTS

We would like to thank Dr. J. J. Sabo and Professor A. F. Kip for many helpful discussions.

[21] G. M. Eliashberg, Zh. Eksperim. i Teor. Fiz. **43**, 1005 (1962) [English transl.: Soviet Phys.—JETP **16**, 780 (1963)].
[22] G. Grimvall, Physik Kondensierten Materie **9**, 283 (1969).
[23] J. Appel, Phys. Rev. Letters **21**, 1164 (1968).

PHYSICAL REVIEW B VOLUME 1, NUMBER 4 15 FEBRUARY 1970

Effects of Off-Diagonal Randomness in the Tight-Binding Model of Random Binary Alloys: Weak-Coupling Limit*

NORMAN F. BERK
Department of Physics and Astronomy, Universtiy of Maryland, College Park, Maryland 20742
(Received 13 October 1969)

The single-band tight-binding model of random binary alloys is studied in the limit of second-order self-consistent perturbation theory, allowing the off-diagonal, as well as the diagonal, matrix elements of the model Hamiltonian to be dependent upon alloy composition. Fluctuations of both types of matrix elements about their configurational averages are assumed to be small but comparable, so that the randomness introduced into both parts of the Hamiltonian must be treated on an equal footing. Only nearest-neighbor hopping between constituent atoms (type A or B) is considered, with the hopping integrals parametrized by the three numbers α, β, and γ for A-A, B-B, and A-B hopping, respectively. The single-particle alloy spectrum and the alloy density of states are obtained from an equation for the effective single-particle self-energy using standard techniques and with the dependence on model parameters explicitly displayed. With the assumption that $\gamma=\frac{1}{2}(\alpha+\beta)$, the theory is found to be rather simply characterized by the wave-vector–dependent displace ment $E_A(\mathbf{k})-E_B(\mathbf{k})$ of the pure constituent spectra $E_A(\mathbf{k})$ and $E_B(\mathbf{k})$.

I. INTRODUCTION

AN important contribution to the one-electron theory of disordered alloys has been Soven's[1] introduction of the coherent potential approximation (CPA), with subsequent development and application to a model alloy Hamiltonian by Soven,[2] and by Velický, Kirkpatrick, and Ehrenreich.[3]

These authors have shown that, with certain limitations, the CPA provides a powerful and elegant means of extending the theory of simple binary alloys beyond the confines of low-order perturbation (or "weak-coupling") theory to the regime of relatively large con-

* Supported in part by the Center for Theoretical Physics, the U. S. Office of Naval Research, and the Advanced Research Projects Agency.
[1] Paul Soven, Phys. Rev. **156**, 809 (1967).
[2] Paul Soven, Phys. Rev. **178**, 1136 (1969).
[3] B. Velický, S. Kirkpatrick, and H. Ehrenreich, Phys. Rev. **175**, 747 (1968).

stituent energy level separations.[2,3] One important limitation to the practical, and even conceptual, utility of the CPA is the requirement that the alloy Hamiltonian be expressible as a sum of single-site Hamiltonian contributions, i.e., that

$$H=\sum_n H_n, \tag{1.1}$$

where H is the alloy Hamiltonian operator and H_n refers to the single site n with regard to both position and constituent occupation. The single-band tight-binding alloy Hamiltonian[2,3]

$$H=\sum_n |n\rangle\epsilon_n\langle n| + \sum_{n\neq m} |m\rangle t_{mn}\langle n| \tag{1.2}$$

meets the condition (1.1) only if the hopping integrals t_{mn} are independent of composition. In (1.2), $|n\rangle$ represents a single atomic orbital at the site n, which may correspond to an atom of either type A or B (we consider only binary alloys). Associated with each orbital is the atomic level $\epsilon_n=\epsilon_A$ or ϵ_B. The off-diagonal matrix elements t_{mn}, which represent the hopping energy, couple sites m and n, each of which may be occupied by an A or B atom. In the approximation used to develop the CPA, the t_{mn} are assumed to be independent of the types of atoms occupying the sites m and n; the off-diagonal part of (1.2) is then periodic, allowing the decomposition of (1.2) into the sum of single-site contributions as in (1.1). The physically important case of alloying constituents which have different bandwidths is, thus, excluded from the model.

The purpose of the present work is to free the model somewhat of the above qualifications on the hopping integrals by allowing both the off-diagonal and diagonal parts of (1.2) to be random. The model Hamiltonian then no longer fits into the single-site approximation, so that a straightforward extension of the coherent potential scheme is ruled out. Instead, attention is focused on the considerably more modest goal of studying the effects of off-diagonal randomness on the weak coupling or perturbative limit, which is appropriate if fluctuations of the matrix elements of (1.2) about their configurational averages are sufficiently small. The perturbative regime has been studied previously,[2–6] of course, but not explicitly with regard to off-diagonal randomness in the model defined by (1.2). Given the role of the restricted form of (1.2) in the development of the CPA, the weak-coupling theory of the extended model illuminates some of the difficulties to be encountered in any attempt to generalize the CPA to the case of off-diagonal randomness, while also providing the appropriate perturbative limit when the effects of both diagonal and off-diagonal randomness are small but not necessarily with respect to each other.

[4] R. H. Parmenter, Phys. Rev. **97**, 587 (1955).
[5] Edward A. Stern, Physics **1**, 255 (1965).
[6] Edward A. Stern, Phys. Rev. **144**, 545 (1966).

The basic formalism of the present work is the same employed in Refs. 2 and 3, except that it is tailored here explicitly to the perturbative regime. The essentials of the formalism are outlined, for completeness, in Sec. II. In Secs. IIIA–IIIB, the theory is worked out specifically for the model Hamiltonian (1.2), assuming that the hopping integrals connect nearest-neighbor sites only. At the outset, no other restriction is set on the off-diagonal part of the Hamiltonian. Eventually, however, in Sec. IIIB, it is assumed for convenience that the A-B hopping integral is the numerical average of the A-A and B-B hopping integrals, an assumption which leads to a simpler characterization of the theory in terms of the energy spectra of the two consituents. The effects of off-diagonal randomness on the single-particle spectrum and density of states of the alloy are then discussed, respectively, in Secs. IIIB and IIIC. Some concluding remarks follow in Sec. IV.

II. FORMALISM

The one-electron equilibrium properties of the random (binary) alloy are derived from the configurational average (denoted by $\langle\ \rangle$) of the Green's-function operator $G(E)$, which satisfies

$$(E-H)G(E)=1. \tag{2.1}$$

Here, H is the alloy Hamiltonian operator given by (1.1),

$$H=\sum_n |n\rangle\epsilon_n\langle n| + \sum_{n\neq m} |m\rangle t_{mn}\langle n|, \tag{2.2}$$

where the $|n\rangle$ represent single atomiclike orbitals associated with atoms of type A or B, as is appropriate, at the site n; the A and B orbitals are not assumed to be equivalent. For a given configuration of A and B atoms, the states

$$|\mathbf{k}\rangle=N^{-1/2}\sum_n e^{i\mathbf{k}\cdot\mathbf{R}_n}|n\rangle, \tag{2.3}$$

while not periodic, are orthonormal provided that

$$\langle m|n\rangle=\delta_{mn}, \tag{2.4}$$

which is taken to be true for the model. In Eq. (2.3), $N=$ total number of sites, $\mathbf{R}_n$ is the position vector of each site, and the summation is over all sites. Equation (2.4) assumes that direct overlap between orbitals on different sites is negligible and that each orbital is normalized to unity over the whole of the crystal; therefore, $\langle\mathbf{k}|\mathbf{k}'\rangle=\delta_{\mathbf{k}\mathbf{k}'}$. For a given configuration, then, Eq. (2.1) has the k representation

$$\langle\mathbf{k}|G(E)|\mathbf{k}'\rangle E-\sum_{\mathbf{q}}\langle\mathbf{k}|H|\mathbf{q}\rangle\langle\mathbf{q}|G(E)|\mathbf{k}'\rangle=\delta_{\mathbf{k}\mathbf{k}'}. \tag{2.5}$$

As a starting approximation, we use the virtual[4] (or averaged) crystal Hamiltonian operator H_0, which is diagonal in the k representation and defined by

$$H_0=\sum_{\mathbf{k}} |\mathbf{k}\rangle\bar{E}(\mathbf{k})\langle\mathbf{k}|, \tag{2.6}$$

with

$$\bar{E}(\mathbf{k})=\langle\langle\mathbf{k}|H|\mathbf{k}\rangle\rangle. \tag{2.7}$$

Substituting H_0 into (2.5) defines the Green's function $\langle\mathbf{k}|G_0(E)|\mathbf{k}'\rangle=\delta_{\mathbf{k}\mathbf{k}'}G_0(E,\mathbf{k})$, where

$$G_0(E,\mathbf{k})=(E-\bar{E}(\mathbf{k}))^{-1}. \tag{2.8}$$

Now setting $H=H_0+H-H_0$ and using (2.6)–(2.8), Eq. (2.5) becomes

$$\langle\mathbf{k}|G(E)|\mathbf{k}'\rangle=\delta_{\mathbf{k}\mathbf{k}'}G_0(E,\mathbf{k})+G_0(E,\mathbf{k})\textstyle\sum_{\mathbf{q}}\langle\mathbf{k}|V|\mathbf{q}\rangle\langle\mathbf{q}|G(E)|\mathbf{k}'\rangle, \tag{2.9}$$

with

$$V=H-H_0. \tag{2.10}$$

The alloy Green's function of physical interest is defined by the relations

$$\langle\langle\mathbf{k}|G(E)|\mathbf{k}'\rangle\rangle=\delta_{\mathbf{k}\mathbf{k}'}G(E,\mathbf{k}) \tag{2.11}$$

and

$$G(E,\mathbf{k})=(E-\bar{E}(\mathbf{k})-\Sigma(E,\mathbf{k}))^{-1}, \tag{2.12}$$

where $\Sigma(E,\mathbf{k})$ is the effective single-particle self energy for the alloy. An expression for $\Sigma(E,\mathbf{k})$ is obtained by iterating Eq. (2.9) and taking the configurational average of both sides. Using (2.11) and (2.12), one then finds, to second order in the matrix elements of V,

$$\Sigma(E,\mathbf{k})=\textstyle\sum_{\mathbf{q}}\langle\langle\mathbf{k}|V|\mathbf{q}\rangle\langle\mathbf{q}|V|\mathbf{k}\rangle\rangle G_0(E,\mathbf{q})+\cdots. \tag{2.13}$$

The first-order contribution $\langle\langle\mathbf{k}|V|\mathbf{k}\rangle\rangle$ vanishes identically since the perturbation is referred to the configurationally averaged lattice.

According to (2.13), $\mathrm{Im}\Sigma(E+i0^+,\mathbf{k})$, and, hence, the spectral density $-\pi\,\mathrm{Im}G(E+i0^+,\mathbf{k})$ of the Green's function vanishes outside the band defined by the virtual-crystal Hamiltonian H_0, while the energy shift implicit in $\mathrm{Re}\Sigma(E+i0^+,\mathbf{k})$ extends the alloy spectrum beyond the virtual-crystal band edges. The use of the self-energy expression given by (2.13), therefore, does not lead to a self-consistent determination of the bounds of the alloy spectrum. In the present context, the requirement of self-consistency stipulates that the starting approximation to the configurationally averaged alloy Green's function be so chosen that, to the desired order of calculation, perturbative corrections vanish, i.e., that the perturbation be referenced to the self-determined effective alloy medium.[2,3] Thus, the necessary generalization of (2.13) is obtained by replacing H_0 by H_0+K, where K is to be determined but can be taken to be diagonal in the k representation; $\langle\mathbf{k}|K|\mathbf{k}'\rangle\equiv\delta_{\mathbf{k}\mathbf{k}'}\times\Sigma'(E,\mathbf{k})$. With this replacement, the starting approximation for the Green's function becomes $G_0(E,\mathbf{k})=[E-\bar{E}(k)-\Sigma'(E,\mathbf{k})]^{-1}$, and the operator V in (2.10) becomes $V-K$. Proceding as before and iterating Eq. (2.9) in powers of $V-K$, one obtains a relationship between $\Sigma(E,\mathbf{k})$ and $\Sigma'(E,\mathbf{k})$. The self-consisting requirement $\Sigma'=\Sigma$ then leads to

$$\Sigma(E,\mathbf{k})=\sum_{\mathbf{q}}\langle|\langle\mathbf{k}|V|\mathbf{q}\rangle|^2\rangle G(E,\mathbf{q})+\cdots, \tag{2.14}$$

where $G(E,\mathbf{k})$ is given by (2.12) and where the matrix elements of K, which are at least second-order in V, have been neglected in the average $\langle|\langle\mathbf{k}|V-K|\mathbf{q}\rangle|^2\rangle$; these vertex corrections contribute to $\Sigma(E,\mathbf{k})$, and, hence, to the poles of $G(E,\mathbf{k})$, only beyond second-order in V. In the analysis which follows in Sec. III, where the average appearing in (2.14) is calculated and the summation performed, only contributions which lead to second-order corrections to the poles of $G(E,\mathbf{k})$ are retained.

III. APPLICATION TO MODEL

A. Virtual Crystal

In this subsection, the average $\langle|V|^2\rangle$ which appears in (2.14) is obtained explicitly in terms of the model parameters. First, however, the model is defined in further detail. As discussed in Sec. I, the off-diagonal hopping matrix elements t_{mn} couple orbitals of either type A or B on the two sites m and n. For any two (fixed) sites, the t_{mn} are taken to constitute a set of three real numbers depending upon how the sites in question are occupied:

$$\begin{aligned} t_{mn}&=\alpha_{mn}, && \text{both } A \text{ atoms}\\ &=\beta_{mn}, && \text{both } B \text{ atoms}\\ &=\gamma_{mn}, && \text{one } A, \text{ one } B \text{ atom}. \end{aligned} \tag{3.1}$$

Formally, the α_{mn}, β_{mn}, and γ_{mn} can be considered as parameters which, to some extent, are adjustable. For example, it is tacitly being assumed that the lattice spacing is unchanged by alloying, allowing for a sensible definition of a rigid periodic empty lattice. Real lattice distortion may be accommodated to some degree by the values chosen for the hopping parameters, or by allowing them to have an appropriate concentration dependence. For the purposes here, however, the simplest assumptions are made, including the restriction to nearest-neighbor hopping interactions only. Additionally, the empty lattice is assumed to have cubic symmetry. The explicit subscripting of α, β, and γ, is, hence, no longer necessary. The configurational average of t_{mn} over the random occupations of any two nearest-neighbor sites is then simply

$$t\equiv\langle t_{mn}\rangle=x^2\alpha+y^2\beta+2xy\gamma, \tag{3.2}$$

where $x=N_A/N$ is the concentration of type A atoms and $y=N_B/N=1-x$ is the concentration of type B atoms. The factor of 2 in Eq. (3.2) accounts for the two ways in which the nearest-neighbor sites can be occupied by different atoms. One can also write Eq. (3.2) as

$$t=xt_A+yt_B, \tag{3.3a}$$

where

$$t_A = x\alpha + y\gamma, \tag{3.3b}$$

$$t_B = x\gamma + y\beta. \tag{3.3c}$$

The "partial averages" t_A and t_B are obtained by averaging over the occupation of one site, fixing the occupation of the other by either an A atom (t_A) or a B atom (t_B). The partial averages are convenient devices for performing two (or multiple) site averages over products of matrix elements, such as occur in Subsec. IIIB. The averaged diagonal matrix element of (2.2) is simply

$$\epsilon \equiv \langle \epsilon_n \rangle = x\epsilon_A + y\epsilon_B. \tag{3.4}$$

Combining these results with the definitions in Sec. II, we have, for the virtual crystal energy,

$$\bar{E}(\mathbf{k}) = \epsilon + W(\mathbf{k}), \tag{3.5}$$

with

$$W(\mathbf{k}) = t \sum_{\text{n.n.}} e^{i\mathbf{k}\cdot\rho} \equiv tB(\mathbf{k}). \tag{3.6}$$

The sum in (3.6) is over nearest-neighbor lattice vectors $\boldsymbol{\rho}$, and $B(\mathbf{k})$ is the nearest-neighbor structure factor: $-Z \leqslant B(\mathbf{k}) \leqslant Z$, Z being the number of nearest-neighbor sites. With the sign conventions in (2.2), the hopping matrix elements are negative numbers. The half-bandwidth of the virtual-crystal band is therefore

$$w = -Zt, \tag{3.7}$$

a positive number. Thus, the lowest-order effect of off-diagonal randomness in (2.2) is to introduce a concentration-dependent alloy bandwidth, which, according to (3.2), varies parabolically in either x or y; a special case results if $2\gamma = \alpha + \beta$, giving a linear dependence of w on x and y. When the three parameters are equal, it follows from (3.2) or (3.3), and the identity $x+y=1$, that t is then independent of concentration.

B. Weak-Coupling Correction

Combining the various definitions introduced in Secs. II and IIIA, the matrix element $\langle \mathbf{k}|V|\mathbf{q}\rangle$ which appears in Eq. (2.14) takes on the form

$$\langle \mathbf{k}|V|\mathbf{q}\rangle = N^{-1} \sum_n e^{i(\mathbf{q}-\mathbf{k})\cdot\mathbf{R}_n} [v_n + \sum_{m(n)} e^{-i\mathbf{k}\cdot\rho_{mn}} h_{mn}], \tag{3.8}$$

where

$$v_n = \epsilon_n - \epsilon \tag{3.9}$$

and

$$h_{mn} = t_{mn} - t. \tag{3.10}$$

The symbol $\sum_{m(n)}$ indicates a sum over sites m which are nearest neighbors to the site indicated in parentheses, and $\boldsymbol{\rho}_{mn} = \mathbf{R}_m - \mathbf{R}_n$ is the appropriate nearest-neighbor position vector. From the definitions of ϵ and t in (3.4) and (3.2), respectively, it follows that

$$\langle v_n \rangle = 0 \tag{3.11a}$$

and

$$\langle h_{mn} \rangle = 0. \tag{3.11b}$$

Therefore, keeping in mind that the exponential factors in (3.8) are purely geometric, we have

$$\langle\langle \mathbf{k}|V|\mathbf{q}\rangle\rangle = 0. \tag{3.11c}$$

Using $|\langle \mathbf{k}|V|\mathbf{q}\rangle|^2 = \langle \mathbf{k}|V|\mathbf{q}\rangle\langle \mathbf{q}|V|\mathbf{k}\rangle$ and Eq. (3.8), we have, for the averaged square of the matrix element,

$$\begin{aligned}\langle |\langle \mathbf{k}|V|\mathbf{q}\rangle|^2 \rangle = N^{-2} \sum_{n,n'} e^{i(\mathbf{q}-\mathbf{k})\cdot(\mathbf{R}_n - \mathbf{R}_{n'})} \\ \times [\langle v_n v_{n'} \rangle + \sum_{m'(n')} e^{-i\mathbf{q}\cdot\rho_{m'n'}} \langle v_n h_{m'n'} \rangle \\ + \sum_{m(n)} e^{-i\mathbf{k}\cdot\rho_{mn}} \langle v_{n'} h_{mn} \rangle \\ + \sum_{m(n)} \sum_{m'(n')} e^{-i\mathbf{k}\cdot\rho_{mn}} e^{-i\mathbf{q}\cdot\rho_{m'n'}} \langle h_{mn} h_{m'n'} \rangle].\end{aligned} \tag{3.12}$$

Three distinct averages are involved in the analysis of Eq. (3.12). In each case, the average of the product factorizes into the product of the averages when the sets of indices labeling each factor share no site in common. Thus, recalling (3.11),

$$\begin{aligned}\langle v_n v_{n'} \rangle &= \langle v_n \rangle \langle v_{n'} \rangle = 0, \qquad n \neq n' \\ \langle v_n h_{m'n'} \rangle &= \langle v_n \rangle \langle h_{m'n'} \rangle = 0, \quad n \neq m' \text{ or } n' \\ \langle h_{mn} h_{m'n'} \rangle &= \langle h_{mn} \rangle \langle h_{m'n'} \rangle = 0,\end{aligned} \tag{3.13}$$

unless the pairs (m,n) and $(m'n')$ share a common index. The nonvanishing averages are represented by

$$\begin{aligned}\langle v_n v_{n'} \rangle &= \langle v^2 \rangle, \quad n = n' \\ \langle v_n h_{m'n'} \rangle &= \langle vh \rangle, \quad n = m' \text{ or } n' \\ \langle h_{mn} h_{m'n'} \rangle &= \langle hh \rangle, \quad \text{one common index} \\ &= \langle h^2 \rangle, \quad \text{two common indices.}\end{aligned} \tag{3.14}$$

The reduction of (3.12) using (3.13) and (3.14) is straightforward, although somewhat lengthy. The simplest program is to take each of the four averages in turn, applying the rules of (3.14) to all possible distinct cases which yield nonvanishing contributions. The restrictions on the indices encompassed in (3.14) lead, in every case, to summations over nearest-neighbor lattice vectors which can be written in terms of the structure factor, (3.6), or products of structure factors. The average $\langle v_n v_{n'} \rangle$ gives a single term, corresponding to the case $n=n'$. The two averages $\langle v_n h_{m'n'} \rangle$ and $\langle v_{n'} h_{mn} \rangle$ lead to equal contributions, each involving two terms. The most involved case, of course, is the average $\langle h_{mn} h_{m'n'} \rangle$, which can be written as the sum of six terms. It is worthwhile pointing out that while the hopping-matrix element t_{mn} connects only nearest-neighbor sites, the second-order scattering via the product hGh involves sites outside the nearest-neighbor shell of any given site. In a typical scattering process, for example, an electron can make successive hops (as distinct from propagation via the Green's function—the hopping is an interaction) from a given atom to a nearest neighbor, and then from there—after a "closed-loop" propaga-

tion—to an atom outside the nearest-neighbor shell. Such multiple hoppings generate a large number of terms in the perturbative development of the alloy Green's function. Fortunately, the number of terms in second order is manageable, and the results of the above procedure can be put into the form

$$\langle|\langle\mathbf{k}|V|\mathbf{q}\rangle|^2\rangle = N^{-1}[\langle v^2\rangle + 2\langle vh\rangle(B(\mathbf{k})+B(\mathbf{q})) + \langle hh\rangle^2(B(\mathbf{k})+B(\mathbf{q}))^2 + (\langle h^2\rangle - \langle hh\rangle)(Z+B(\mathbf{k}+\mathbf{q}))]. \quad (3.15)$$

The single-site and two-site averages appearing in Eq. (3.15) are determined from the definitions (3.1), (3.10), and (3.14); the partial averaging mentioned in Sec. IIIA helps simply the algebra. We then have, in terms of the model parameters,

$$\langle v^2\rangle = xy(\epsilon_A-\epsilon_B)^2, \quad (3.16a)$$

$$\langle vh\rangle = xy(\epsilon_A-\epsilon_B)(t_A-t_B), \quad (3.16b)$$

$$\langle hh\rangle = xy(t_A-t_B)^2, \quad (3.16c)$$

$$\langle h^2\rangle - \langle hh\rangle = (xy)^2(\alpha+\beta-2\gamma)^2, \quad (3.16d)$$

where t_A and t_B are given in (3.3). Noting that the three averages in (3.16a)–(3.16c) are products of common factors, the result in (3.15) can be written as

$$\langle|\langle\mathbf{k}|V|\mathbf{q}\rangle|^2\rangle = xyN^{-1}[\epsilon_A-\epsilon_B+(t_A-t_B)(B(\mathbf{k})+B(\mathbf{q}))]^2 + (xy)^2(\alpha+\beta-2\gamma)^2(Z+B(\mathbf{k}+\mathbf{q})). \quad (3.17)$$

The self-energy equation, (2.14), can now be reduced using (3.17), (2.12), and Eqs. (3.5)–(3.7) for $\bar{E}(\mathbf{q})$. The q summation in Eq. (2.14), then, involves products of the structure factors appearing in (3.17) with the Green's function $G(E,\mathbf{q})$. Because of the assumed cubic symmetry, these sums can be done exactly to second order using the techniques found in Sec. III of the paper by Wolfram and Callaway.[7] The result, which is a bit cumbersome, is shown in the Appendix. Rather than using this result, however, we note that (3.17) takes on a simpler more intuitive form if the hopping integrals are assumed to satisfy the relation

$$\gamma = \tfrac{1}{2}(\alpha+\beta). \quad (3.18)$$

The condition in (3.18) is not unreasonable in the limit that $\alpha\simeq\beta\simeq\gamma$ and could be viewed as resulting from an approximation which neglects the difference between the orbital wave functions of the A and B atoms in the hopping integrals in comparison to the difference between the atomic potentials. Thus, given (3.18), Eq. (3.17) becomes

$$\langle|\langle\mathbf{k}|V|\mathbf{q}\rangle|^2\rangle = xy(4N)^{-1}[\Delta(\mathbf{k})+\Delta(\mathbf{q})]^2, \quad (3.19)$$

where

$$\Delta(\mathbf{k}) = E_A(\mathbf{k}) - E_B(\mathbf{k}), \quad (3.20)$$

with

$$E_A(\mathbf{k}) = \epsilon_A + W_A(\mathbf{k}), \quad (3.21a)$$

$$E_B(\mathbf{k}) = \epsilon_B + W_B(\mathbf{k}). \quad (3.21b)$$

$E_A(\mathbf{k})$ and $E_B(\mathbf{k})$ are the Bloch energies for the pure crystals of A atoms only and B atoms only, respectively; $W_A(\mathbf{k})=\alpha B(\mathbf{k})$ and $W_B(\mathbf{k})=\beta B(\mathbf{k})$. The half-bandwidths for the two pure systems are $w_A=-Z\alpha$ and $w_B=-Z\beta$. The half-bandwidth for the virtual crystal (3.7) becomes, upon combining (3.2) and (3.7) with (3.18),

$$w = xw_A + yw_B. \quad (3.22)$$

We then have, for the virtual crystal energy (3.5),

$$\bar{E}(\mathbf{k}) = xE_A(\mathbf{k}) + yE_B(\mathbf{k}). \quad (3.23)$$

Thus, with the condition in (3.18), the virtual crystal energy becomes simply the concentration weighted average of the Bloch energies for the two constituent crystals. The result in (3.19) can be compared to the equivalent expression obtained within the single-site approximation discussed in Sec. I. In the latter case, the bandwidths of the two constituents are the same, $w_A=w_B=w$, so that $\Delta(\mathbf{k})=\epsilon_A-\epsilon_B$ measures the relative displacement of the two equivalent bands, which is the same at all points on the Brillouin zone. The right side of Eq. (3.19) then becomes equal to $xy(\epsilon_A-\epsilon_B)^2$, independent of k vector. In the somewhat more general case where the constituent bands have the same structure factor but different widths, the relative displacement, as given by $\Delta(\mathbf{k})$, varies throughout the zone. Subject to (3.18), this momentum-dependent displacement enters the weak-coupling theory in a simple way. With (3.19), the self-energy equation, (2.14) now becomes

$$\Sigma(E,\mathbf{k}) = xy(4N)^{-1}\sum_{\mathbf{q}} \frac{[\Delta(\mathbf{k})+\Delta(\mathbf{q})]^2}{E-\bar{E}(\mathbf{q})-\Sigma(E,\mathbf{q})}. \quad (3.24)$$

Introducing the dimensionless variables

$$\omega = (E-\epsilon)/w, \quad (3.25a)$$

$$\tilde{\omega}(\mathbf{k}) = (\bar{E}(\mathbf{k})-\epsilon)/w, \quad (3.25b)$$

$$\delta = xy(\epsilon_A-\epsilon_B)^2/w^2, \quad (3.26)$$

$$\lambda = (w_A-w_B)/(\epsilon_A-\epsilon_B), \quad (3.27)$$

and using the relation

$$\Delta(\mathbf{q}) = (\epsilon_A-\epsilon_B)[1+\lambda\tilde{\omega}(\mathbf{q})], \quad (3.28)$$

which follows (3.20)–(3.23), Eq. (3.24) can be written, to second order,

$$\Sigma(\omega,\mathbf{k}) = \delta\{[1+\lambda\tilde{\omega}(\mathbf{k})+\tfrac{1}{2}(\omega-\tilde{\omega}(\mathbf{k}))]^2G(\omega) - \lambda[1+\lambda\tilde{\omega}(\mathbf{k})+\tfrac{1}{4}\lambda(\omega-2\tilde{\omega}(\mathbf{k}))]\}, \quad (3.29)$$

[7] Thomas Wolfram and Joseph Callaway, Phys. Rev. **130**, 2207 (1963).

where

$$G(\omega)=wG(E)=N^{-1}\sum_{\mathbf{k}}[\omega-\bar{\omega}(\mathbf{k})-\Sigma(\omega,\mathbf{k})]^{-1}, \quad (3.30)$$

and

$$\Sigma(\omega,\mathbf{k})=w^{-1}\Sigma(E,\mathbf{k}). \quad (3.31)$$

With the variables ω and $\bar{\omega}(\mathbf{k})$, the energies in (3.29) are measured conveniently with respect to the center of the virtual crystal band $\epsilon=x\epsilon_A+y\epsilon_B$ and normalized to the virtual crystal half-bandwidth, $w=xw_A+yw_B$. Thus, recalling from (3.5)–(3.7) that the virtual crystal energy $\bar{E}(\mathbf{k})$ has the limiting values $\epsilon-w\leq\bar{E}(\mathbf{k})\leq\epsilon+w$, it follows that $-1\leq\bar{\omega}(\mathbf{k})\leq 1$. The quantity δ, (3.26), characterizes the weak-coupling limit in the single-site approximation, as discussed above, while the parameter λ, (3.27), measures the difference between the half-bandwidths of the two constituent bands relative to their displacement $\epsilon_A-\epsilon_B$. With the aid of (3.20) and (3.28), one can use the sign and magnitude of λ to distinguish between various dispositions of the constituent bands when both are compared on the same energy scale. Positive values of λ correspond to situations in which the lower edges of the symmetric A and B bands lie closer together than the upper edges. Negative λ corresponds to the opposite case, the upper edges lying closer together than the lower edges. For $\lambda=\pm 1$, the lower (upper) edges are coincident, while for $|\lambda|>1$, one band completely overlaps the other. Since, according to (3.28), the displacement $\Delta(\mathbf{k})=E_A(\mathbf{k})-E_B(\mathbf{k})$ is unaltered if the signs of λ and $\bar{\omega}(\mathbf{k})$ are simultaneously reversed, it is sufficient in what follows to consider only positive values of λ; for $\lambda<0$, the appropriate behavior can be inferred by changing the sign of $\bar{\omega}(\mathbf{k})$ or, equivalently, by interchanging the upper and lower parts of the alloy band.

Now, using (3.29), an approximate single-particle alloy spectrum can be obtained from the poles of the analytic continuation of summand in (3.30) into the lower half complex ω plane:

$$\omega=\bar{\omega}(\mathbf{k})+\Sigma(\omega,\mathbf{k}). \quad (3.32)$$

The real part of (3.32) gives the dispersion relation

$$\omega_{\mathbf{k}}\simeq\bar{\omega}(\mathbf{k})+\delta F_0(\bar{\omega}(\mathbf{k})), \quad (3.33)$$

where

$$F_0(\bar{\omega}(\mathbf{k}))=[1+\lambda\bar{\omega}(\mathbf{k})]^2\,\mathrm{Re}G_0(\bar{\omega}(\mathbf{k})+i0^+) -\lambda[1+\tfrac{3}{4}\lambda\bar{\omega}(\mathbf{k})], \quad (3.34)$$

and where we have taken[8]

$$\mathrm{Re}G(\bar{\omega}(\mathbf{k})+i0^+)\simeq\mathrm{Re}G_0(\bar{\omega}(\mathbf{k})+i0^+) =\mathrm{P.P.}\sum_{\mathbf{q}}[\bar{\omega}(\mathbf{k})-\bar{\omega}(\mathbf{q})]^{-1}.$$

The function $\frac{1}{2}F_0(\bar{\omega}(\mathbf{k}))$ is plotted in Figs. 1 and 2 for several positive values of λ and for two crystal models. The nearest-neighbor simple-cubic model is used in Fig. 1 with values for $\mathrm{Re}G_0(\bar{\omega}(\mathbf{k}))$ obtained from Wolfram

[8] The symbol P. P. stands for "principal part."

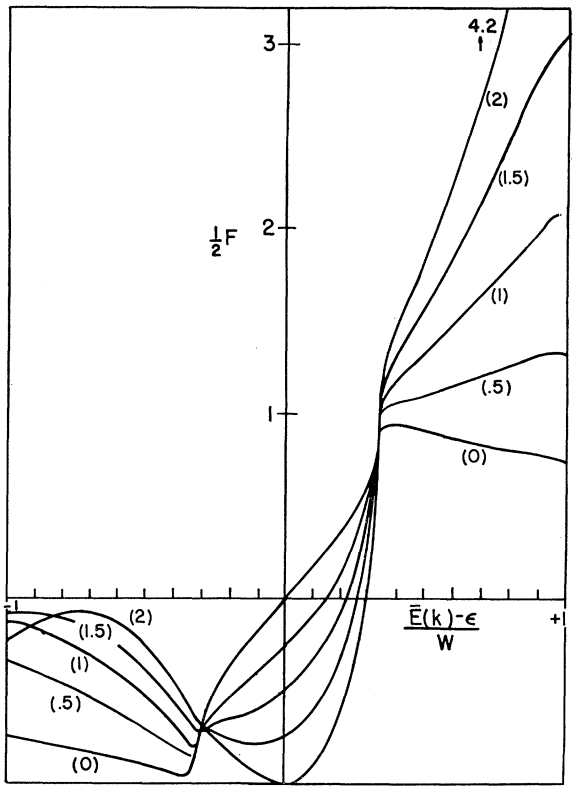

FIG. 1. Second-order correction to virtual crystal spectrum divided by 2δ for simple-cubic model. The curves are labeled by the λ values; 0, 0.5, 1, 1.5, and 2. The order of labeling in the central portion of the figure is the inverse of that near the ends, the $\lambda=0$ curve passing through the origin.

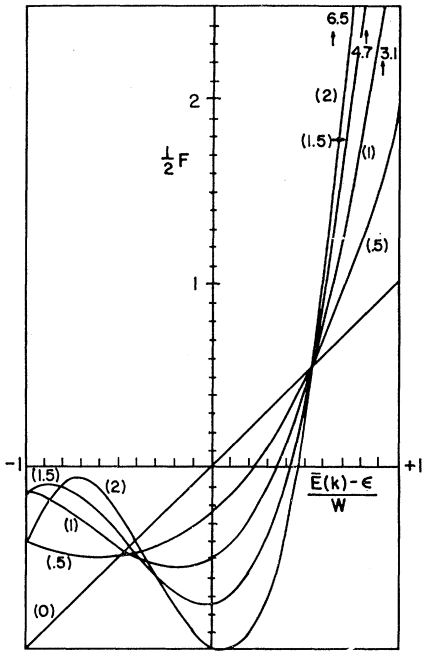

FIG. 2. Second-order correction to virtual crystal spectrum divided by 2δ for "elliptical" model for $\lambda=0$, 0.5, 1, 1,5, and 2.

and Calloway.[7] In Fig. 2, we use the "elliptical" model employed by Velický *et al.*,[3] which gives simply $\mathrm{Re}G_0(\tilde{\omega}(\mathbf{k}))=2\tilde{\omega}(\mathbf{k})$. The latter model is also employed in Subsec. C, where the defining relations are given by (3.42)–(3.43). The corresponding curves for negative λ can be obtained by noting that $F_0(\tilde{\omega};\lambda)=-F_0(-\tilde{\omega},-\lambda)$. Both sets of curves show that for $\lambda\neq 0$ the spectrum tends to lie closer to the virtual crystal limit $\tilde{\omega}_{\mathbf{k}}=\tilde{\omega}(\mathbf{k})$ in the regions of the band characterized by the smaller values of $\Delta(\mathbf{k})/w$, (3.28), while in the regions of larger $\Delta(\mathbf{k})/w$—i.e., near the top of the band for $\lambda>0$—the departure from the virtual-crystal result is markedly enhanced. The gradient of the spectrum $\nabla_{\mathbf{k}}\omega_{\mathbf{k}}\simeq[1+\delta F'(\tilde{\omega}(\mathbf{k}))]\nabla_{\mathbf{k}}\tilde{\omega}(\mathbf{k})$ is correspondingly reduced relative to $\nabla_{\mathbf{k}}\tilde{\omega}(\mathbf{k})$ in the region of small $\Delta(\mathbf{k})/w$ and strongly enhanced where $\Delta(\mathbf{k})/w$ is larger, as can be inferred from the figures.

The imaginary part of (3.32) gives rise to a spectral width which, neglecting for the moment the refinements of self consistency, can be written as

$$\Gamma_{\mathbf{k}}\simeq xy\pi[\Delta(\mathbf{k})/w]^2\rho_0(\tilde{\omega}(\mathbf{k})), \tag{3.35}$$

where $\pi\rho_0(\tilde{\omega}(\mathbf{k}))=-\mathrm{Im}G_0(\tilde{\omega}(\mathbf{k})+i0^+)$ is the density of states of the symmetric virtual crystal band. The level width $\Gamma_{\mathbf{k}}$ is, thus, particularly sensitive to the k dependence of the separation $E_A(\mathbf{k})-E_B(\mathbf{k})$.

C. Density of States

The alloy density of states is obtained from the standard formula

$$\pi\rho(\omega)=-\mathrm{Im}G(\omega+i0^+),\quad \omega \text{ real} \tag{3.36}$$

once equations (3.24)–(3.30) have been solved. The dominant contribution to the density of states comes from the neighborhood of the poles of the summand of (3.30). Neglecting contributions to these poles which are beyond second order allows us to approximate (3.30) by

$$G(\omega)\simeq Z_1^{-1}(\omega)G_0(\omega-\Sigma(\omega)), \tag{3.37}$$

with

$$G_0(\omega)=N^{-1}\sum_{\mathbf{k}}(\omega-\tilde{\omega}(\mathbf{k}))^{-1}, \tag{3.38}$$

$$\Sigma(\omega)=\Sigma(\omega,\mathbf{k})\,|_{\tilde{\omega}(\mathbf{k})=\omega}, \tag{3.39}$$

where

$$\begin{aligned} Z_1(\omega)&=1+\partial\Sigma(\omega,\mathbf{k})/\partial\tilde{\omega}(\mathbf{k})\,|_{\tilde{\omega}(\mathbf{k})=\omega}\\ &=1+\lambda\delta[(1+\lambda\omega)G_0(\omega-\Sigma(\omega))-\tfrac{1}{2}\lambda], \end{aligned} \tag{3.40}$$

using (3.29). The Green's function $G(\omega)$, (3.37), is, thus, known once $\Sigma(\omega)$, (3.39), is known. The required equation for $\Sigma(\omega)$ is obtained from (3.29), which gives, to the desired order,

$$\Sigma(\omega)=\delta[(1+\lambda\omega)^2G_0(\omega-\Sigma(\omega))-\lambda(1+\tfrac{3}{4}\lambda\omega)]. \tag{3.41}$$

For actual cubic structures, (3.41) must be solved numerically. With the model employed by Velický *et al.*, however, the equation can be made algebraic and readily solved. Thus, we take[3]

$$G_0(\omega)\equiv 2[\omega-(\omega^2-1)^{1/2}], \tag{3.42}$$

which, using (3.36), corresponds to a virtual crystal band characterized by the density of states function

$$\begin{aligned} \rho_0(\omega)&=2\pi^{-1}(1-\omega^2)^{1/2}, && |\omega|\leq 1\\ &=0, && |\omega|>1. \end{aligned} \tag{3.43}$$

The function $\rho_0(\omega)$ is symmetric about the center of the virtual crystal band $\omega=0$ and has the typical square root singularity at the virtual crystal-band edges $\omega=\pm 1$, [cf. (3.25b)].

Following Velický *et al.*, (3.42) can be inverted to express $\Sigma(\omega)$ in terms of $G_0(\omega-\Sigma(\omega))$ and the relation which results substituted into Eq. (3.41) to yield a quadratic equation for the Green's function. The physical solution of this equation, which gives a positive density of states, is then combined with Eqs. (3.36), (3.37), and (3.40) to give for the density of states $\rho(\omega)\equiv\rho(\omega;\lambda)$:

$$\begin{aligned} \pi\rho(\omega;\lambda)=\tfrac{1}{2}\{1+\lambda\delta[\lambda-8\omega(1+\lambda\omega)]\}\\ \times[4C(\omega;\lambda)-B^2(\omega;\lambda)]^{1/2}, \end{aligned} \tag{3.44}$$

for $4C-B^2\geqslant 0$,

$$\pi\rho(\omega;\lambda)=0 \quad \text{for} \quad 4C-B^2<0,$$

where

$$B(\omega;\lambda)=-4\omega[1-4\delta(1+\lambda\omega)^2]-4\lambda\delta(1+\tfrac{3}{4}\lambda\omega) \tag{3.45a}$$

and

$$C(\omega;\lambda)=4[1-4\delta(1+\lambda\omega)]. \tag{3.45b}$$

For the case $\lambda=0$, we have, from (3.44) and (3.45),

$$\begin{aligned} \pi\rho(\omega;0)&=2[1-4\delta-\omega^2(1-4\delta)^2]^{1/2}\\ &=2(1-4\delta)[1+4\delta-\omega^2]^{1/2},\quad \delta\ll 1. \end{aligned} \tag{3.46}$$

Although (3.46) was obtained for $\lambda=0$, the normalization of the energy variable ω can still be taken as $w=xw_A+yw_B$ with $w_A\neq w_B$. Thus, $\pi\rho(\omega;0)$ is the self-consistent weak-coupling result in the single-site approximation[3] with the effects of off-diagonal randomness included only in lowest order. Comparison with (3.43) shows the only effect in this limit to be a scale change, the virtual-crystal half-bandwidth being enhanced by the factor $1+2\delta$. The second-order effects of off-diagonal randomness on $\rho(\omega;\lambda)$ can be more readily seen by subtracting out the contribution of $\rho(\omega;0)$. Thus, in Fig. 3, we show the magnified difference $10\pi[\rho(\omega;\lambda)-\rho(\omega;0)]$ for several positive values of λ and with $\delta=0.01$. For negative values of λ, one can use the symmetry relation

$$\rho(\omega;\lambda)=\rho(-\omega;-\lambda), \tag{3.47}$$

which follows, for example, from (3.44), but more generally, from (3.36)–(3.41). The pronounced peaks at the end points of the curves in Fig. 3 result from an asymmetric shift of the alloy band toward higher energies relative to the band characterized by $\rho(\omega;0)$, the shift being larger at the upper edge, particularly as λ increases

(for fixed δ) through the range shown [cf. Subsec. B, Figs. 1 and 2]. The curves also show that $\rho(\omega;\lambda)$ is distorted relative to $\rho(\omega;0)$ throughout the band, tending to be enhanced (for $\lambda>0$) in the lower portion and reduced in the upper portion.

The explicit concentration dependence of the theory, which has thus far been suppressed, enters through the parameters ϵ, w, and δ, as given by Eqs. (3.4), (3.22), and (3.26), respectively. In Fig. 4 we plot the density of states $\rho(E;\lambda)=w^{-1}\rho(\omega;\lambda)$ as a function of $E=\epsilon+w\omega$ and the concentration of the type-A constituent for $\lambda=2$ and $\epsilon_A-\epsilon_B=0.2$, all energies being here renormalized to $\frac{1}{2}(w_A+w_B)$. The situation shown, thus, corresponds to the wider type-A (solute) band being centered slightly above the narrower type-B (host) band but completely overlapping it.[9] The zero of energy is taken at the center of the host band. The vertical hash marks along the energy scales indicate the edges of the virtual crystal band, while small arrows mark the extremal edges of the overlapping A and B spectra. Within the resolution of the figure, the lower edge of the alloy band, which lies in the region of small Δ/w, effectively coincides with the virtual crystal edge over the range of concentration, whereas the upper edge is shifted well beyond the top of the virtual crystal band. The distortion evident in the upper part of the band, where Δ/w is large, is entirely the result of the effects of off-diagonal randomness, characterized by the λ dependence of the theory.[10] Similar behavior is exhibited for other values of λ, as indicated by the curves in Fig. 3. Thus, even in the weak-coupling limit, one can expect significant departures from the predictions of the virtual crystal model when constituents having different bandwidths are alloyed.

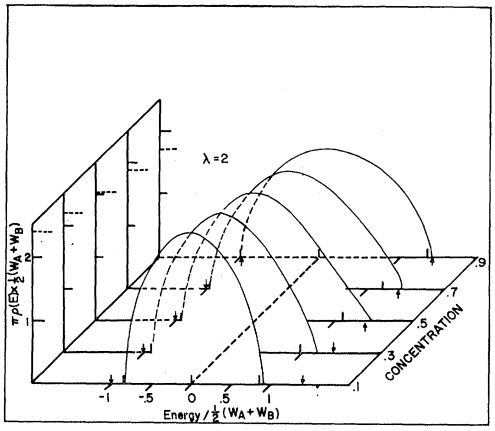

FIG. 4. Density of states for $\lambda=2$ and $\epsilon_A-\epsilon_B=0.2$ in units of $\frac{1}{2}(w_A+w_B)$, and for several values of the concentration of the A-type constituent; the energy origin coincides with the center of the pure B band. Vertical hash marks along the energy axis indicate virtual crystal edges; arrows mark extremal edges of the overlapping constituent bands.

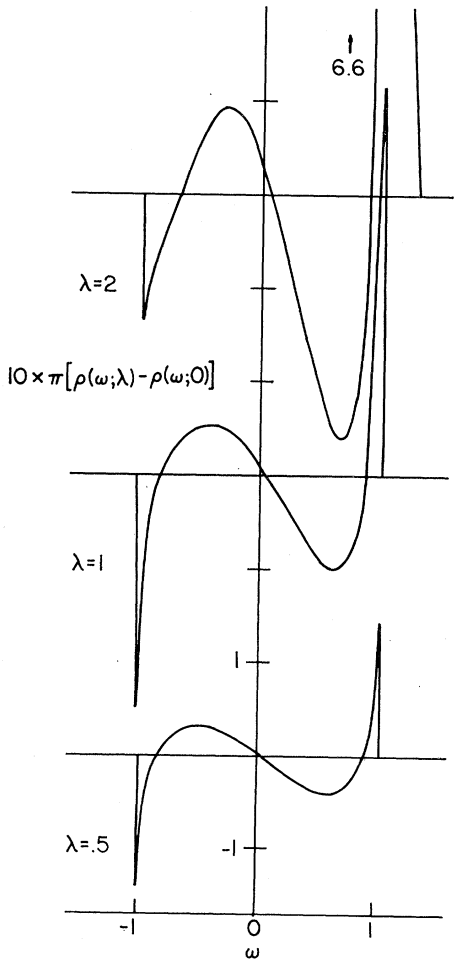

FIG. 3. Magnified comparison of density of states with $\lambda=0$ result for $\delta=0.01$ in the "elliptical" model. The origins of the curves are displaced vertically for display.

IV. CONCLUSION

The aim of this paper has been to indicate how the compositional dependence of the hopping integrals t_{mn} enters into the theory of alloys based on the model Hamiltonian (1.2). Given the assumption that the constituent atoms are randomly distributed throughout the crystal lattice, then, clearly, the randomness introduced into both the diagonal and off-diagonal parts of the Hamiltonian must be treated on an equal footing if the fluctuations in the matrix elements about their average values are comparable. We assumed that these fluctuations were small so that the weak-coupling theory could be employed, but there appears to be no straightforward

[9] Thus, considering only virtual crystal effects, the center of the band shifts linearly as a function of concentration from ϵ_B to ϵ_A while the bandwidth increases linearly from $2w_B$ to $2w_A$.

[10] For $\lambda=-2$ and the same value of $\epsilon_A-\epsilon_B$, the solute band is narrower and centered somewhat below the host band; thus, for this case Fig. 4 can be inverted about both energy and concentration axes. With increasing solute concentration, the virtual crystal band narrows and shifts to lower energy. The departures from virtual crystal behavior are now strongest near the lower edge of the alloy band.

way in which the above approach can be fruitfully extended to arbitrarily higher orders. The essential difficulty, of course, is that, unlike the single-site model, the scattering from individual sites cannot be decoupled; the effective interaction which enters the perturbation theory is inherently nonlocal, connecting neighboring sites through the off-diagonal–hopping-matrix elements. As the iteration of Eq. (2.9) is carried out to higher orders, correspondingly more complicated averages of the matrix elements occur which mix the diagonal and off-diagonal parts of the Hamiltonian. In second order, the simultaneous occupation of two and three sites had to be considered, as described in relation to (3.12). In next order, averages over four sites must be considered, and so on. The perturbative development of the model is, thus, useful only to the extent that the hopping integrals are weakly dependent on composition. If the atomic wave functions of the constituent atoms are very much different from each other, then other approaches are called for.[11]

The essential contribution of the present work is incorporated in the explicit determination of the configurationally averaged square of the matrix element $\langle \mathbf{k}|V|\mathbf{q}\rangle$ given by Eq. (3.17) or, with the approximation in (3.18), by Eq. (3.19). In the latter case, the wave-vector dependence of the theory enters in a particularly simple way through the Bloch energies of the two constituent bands. This in turn leads to a characterization of the results of the theory in terms of the relative displacement $\Delta(\mathbf{k})$ of the constituent spectra, a generalization of the weak-coupling theory of the single-site model, in which case $\Delta(\mathbf{k})=\epsilon_A-\epsilon_B$ is a constant throughout the Brillouin zone. Thus, not surprisingly, the second-order corrections to the virtual crystal approximation are smallest in the neighborhood of small $\Delta(\mathbf{k})$ and largest in the vicinity of large $\Delta(\mathbf{k})$. The location of the alloy band edges and the detailed structure of the density of states near the edges are especially sensitive to the variation of $\Delta(\mathbf{k})$ over the Brillouin zone.

These results, of course, are specific to the model defined by (1.2) and the various simplifying assumptions which have been made, such as the limitation to nearest-neighbor hopping. Nevertheless, they should be indicative of the type of behavior which can be expected from a more sophisticated approach to this complicated problem.

[11] For example, in Ref. 5, the "pseudoatomic limit."

ACKNOWLEDGMENT

The author is grateful to Professor H. Ehrenreich for discussions relating to this work. He has also enjoyed conversations with Dr. B. Velický, Dr. D. Beaglehole, and Dr. D. Falk.

APPENDIX

Using Eqs. (2.8), (3.5), and (3.6) above, and Sec. III1 of Ref. 7, it is straightforward to obtain for a lattice with cubic symmetry

$$N^{-1}\sum_{\mathbf{q}} B(\mathbf{q})G_0(E,\mathbf{q})=-Zw^{-1}g_0(E)\,, \tag{A1}$$

$$N^{-1}\sum_{\mathbf{q}} B^2(\mathbf{q})G_0(E,\mathbf{q})=Z^2w^{-2}(E-\epsilon)g_0(E)\,, \tag{A2}$$

$$N^{-1}\sum_{\mathbf{q}} B(\mathbf{k}+\mathbf{q})G_0(E,\mathbf{q})=Zw^{-2}W(\mathbf{k})g_0(E)\,, \tag{A3}$$

where

$$g_0(E)=(E-\epsilon)G_0(E)-1\,, \tag{A4}$$

$$G_0(E)=N^{-1}\sum_{\mathbf{q}} G_0(E,\mathbf{q})\,, \tag{A5}$$

and $\sum_{\mathbf{k}} B(\mathbf{k})=0$. The effect of replacing $G_0(E;\mathbf{q})$ by $G(E,\mathbf{q})$, (2.12), on the left-hand side of (A1)–(A3) is to make the same replacement on the right-hand side and to give extra terms which are proportional to powers of the self energy; these additional terms are higher-order corrections which must be systematically neglected. Thus, to desired order, substitution of (3.17) into (2.14) gives, using (A1)–(A5) with $G_0\to G$

$$\begin{aligned}\Sigma(E,\mathbf{k})=xy\{&[\epsilon_A-\epsilon_B-Z(t_A-t_B)(E+\bar{E}(\mathbf{k})-2\epsilon)/w]^2\\&+Zxy(\alpha+\beta-2\gamma)^2[1+(E-\epsilon)(\bar{E}(\mathbf{k})-\epsilon)/w^2]\}G(E)\\&+xyZw^{-1}[2(\epsilon_A-\epsilon_B)(t_A-t_B)\\&-Z(t_A-t_B)^2(E+2\bar{E}(\mathbf{k})-3\epsilon)/w\\&-xy(\alpha+\beta-2\gamma)^2(\bar{E}(\mathbf{k})-\epsilon)/w].\end{aligned} \tag{A6}$$